

ORIGINAL RESEARCH PAPER

Investigating the Influence of Doping Graphene with Silicon and Germanium on the Adsorption of Silver (I)

Mohammad Reza Jalali Sarvestani¹, Roya Ahmad^{2,*}

¹ Young Researchers and Elite Club, Yadegar-e-Imam Khomeini (RAH) Shahr-e-Rey Branch, Islamic Azad University, Tehran, Iran

² Department of Chemistry, Yadegar-e-Imam Khomeini (RAH) Shahr-e-Rey Branch, Islamic Azad University, Tehran, Iran

Received: 2018-07-29

Accepted: 2018-10-19

Published: 2019-02-01

ABSTRACT

In this study, the impact of doping graphene with silicon and germanium on the adsorption of Ag⁺ was evaluated by density functional theory for the first time. At the outset, the structures of silver, adsorbents and their derived products at ten different configurations were optimized geometrically. Then, IR and frontier molecular orbital calculations were implemented on them and some important parameters such as adsorption energy, Gibbs free energy changes, enthalpy variations, the thermodynamic equilibrium constant, specific heat capacity, chemical hardness, energy gap, and electrophilicity were obtained and inspected. The achieved results indicate that by doping graphene with silicon and germanium the adsorption process has become more spontaneous, exothermic and experimentally feasible. The influence of temperature on the adsorption procedure was also checked out and the results indicate that 298.15 K is the optimum temperature for the desired process at all of the evaluated configurations. The HOMO-LUMO related parameters reveal that the pure and also doped nano-adsorbents are not appropriate sensing material in the construction of conductometric sensors but they can act as an eminent neutral ion carrier in the development of a potentiometric ion selective electrode for determination of silver (I) cations.

Keywords: Adsorption; Ag⁺; Density functional theory; Graphene

How to cite this article

Jalali Sarvestani MR, Ahmadi R. Investigating the Influence of Doping Graphene with Silicon and Germanium on the Adsorption of Silver (I). J. Water Environ. Nanotechnol., 2019; 4(1): 48-59. DOI: 10.22090/jwent.2019.01.005

INTRODUCTION

Silver is a soft white transition metal with 47 atomic number which is represented by Ag symbol. Ag has the most thermal and electrical conductivity among other metals and its most common oxidation state is Ag (I). This metal is widely utilized in the production of coins, mirrors, electrical devices, pharmaceutical products, cosmetics, jewelry, batteries, catalysts and photographic films [1-3]. Therefore, its discharge in the environment and getting exposure to living organisms is highly probable. And due to the fact that Ag can cause severe and irreversible damages including nausea, diarrhea, shock, respiratory irritation, liver and

kidney malfunctions, skin irritation, cardiovascular disease and different types of cancer for humans, its determination and removal from environmental specimens is extremely significant. The next matter that accentuates the importance of silver removal is the price of this metal [4-6]. Because recycling of Ag can reduce the expenses of the aforementioned industries and increase their increment. In this regards, many studies have been focused on the determination and removal of this toxic and precious metal [7].

Despite the fact that numerous analytical methods such as atomic absorption spectroscopy with both flame and graphite furnace atomizers, inductively coupled atomic emission spectroscopy

* Corresponding Author Email: roya.ahmadi.chem@hotmail.com



This work is licensed under the Creative Commons Attribution 4.0 International License.

To view a copy of this license, visit <http://creativecommons.org/licenses/by/4.0/>.

(ICP-AES) and UV-Visible spectrophotometry have been designed for determination of Ag^+ , but most of them have conspicuous disadvantages that make them undesirable [8-10]. For instance, intricate instrumentation, being expensive and time-consuming analysis procedures are the most problems of the referred methods. Fortunately, as an ideal alternative for the cited analytical techniques, we can refer to electrochemical and thermal sensors because these types of sensors are economical, time-saving, portable, selective, sensitive and straightforward. But the main step in the construction of a sensor is finding an appropriate sensing material [11-13].

In addition, a lot of approaches like electrolysis, precipitation, ion flotation, ion exchange, and membrane separation have been developed for removal of Ag^+ ions. However, these techniques are not thrifty because they are based on the instruments that are extremely expensive [14-16]. Owing to the fact that reducing the expenses of pollutants' removal procedures can play a decisive role in encouraging various industries to paying more attention to environmental issues. Allocating more researches to low-cost methods such as adsorption seems logical [17-20].

On the other hand, graphene which its structure is given in Fig. 1, is a hexagonal lattice of carbon atoms. In this two-dimensional nanostructure, sp^2 hybridized carbon atoms are bonded to each other [21-24]. Owing to the fact that, graphene is a porous carbon substance which has an outstanding specific surface area and unique structure, it has excellent physical and chemical properties for adsorption and removing various

compounds and it is one of the most widely used adsorbents for eliminating environmental pollutants [25-27]. Moreover, its specific electrical features make it an ideal electroactive sensing material for electrochemical detection of various analytes. In this regard, it was decided to evaluate the interaction of silver (I) with graphene and the impact of doping graphene with silicon and germanium on this process by density functional theory for the first time.

COMPUTATIONAL DETAILS

In this study, the structures of Ag^+ , graphene, and Ag-graphene complex were designed primarily by using Gauss View 3.1 and nanotube modeler 1.3.0.3 software. Then, geometrical optimizations, IR and frontier molecular orbital calculations were performed on them via Spartan software. All of the calculations were implemented in the aqueous phase and in the temperature range of 298.15 - 398.15 K at 10° intervals. In order to evaluate the effect of doping graphene with silicon and germanium on the adsorption of silver (I), the central ring of each graphene sheet was doped with silicon, germanium and also both of them (co-doping) in three ortho, meta and para situations. Afterward, the cation was inserted in the same place near the central ring for implementing the mentioned computations. It should be noted that silicon and germanium were chosen as dopant atoms because both of them are in the carbon group at the periodic table and they have similar valence and properties to carbon. The next matter that supports selecting these elements as dopant atoms is that in previous researches,

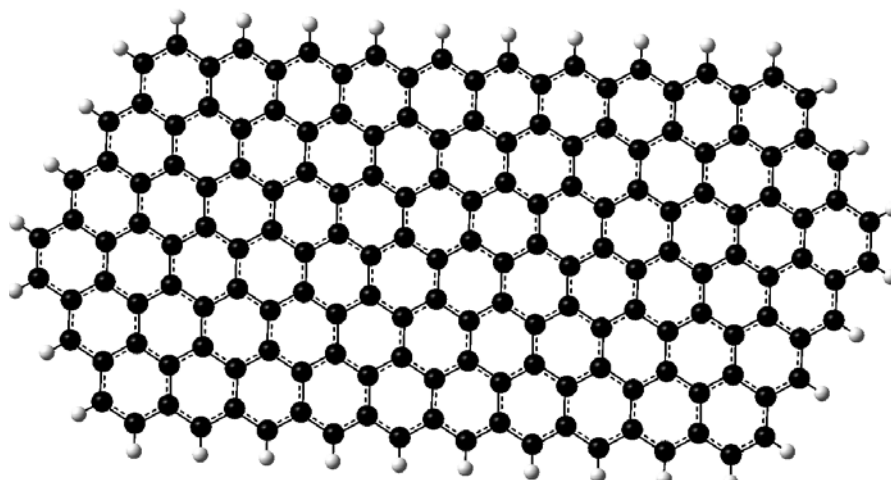
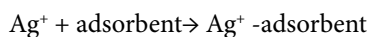


Fig. 1. The chemical structure of graphene

doping graphene with silicon and germanium had led to noteworthy and meaningful results. All calculations were carried out at B3LYP/6-31G(d) level of density functional theory. This basis set was selected because it had produced results which were in good accordance with experimental data in our former researches [27-37]. The studied reaction was as follows:



RESULTS AND DISCUSSION

Naming method

Owing to the fact that adsorption of Ag^+ on the surface of pure and doped graphene was evaluated

in ten different situations. For better and more convenient understanding, each condition is called by an abbreviated name. Therefore, explaining the naming method and abbreviations is essential. In this regards, the naming method is described at the following:

At the first step, the capability of the pure graphene which was consisted of only carbon atoms in the adsorption of the studied contaminant was investigated. The pure graphene is shown as PG in this paper and its derivative with silver is demonstrated by Ag-PG abbreviation.

Then the graphene was doped with silicon at three ortho, meta and para circumstances. As it can be seen in Figs. 2 and 3, the dopant elements are

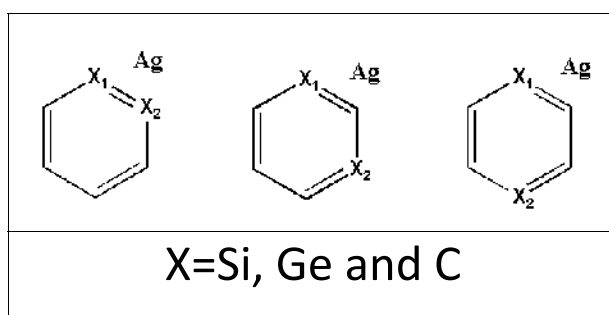


Fig. 2. The location and number of the dopant elements in the central ring of the graphene at three ortho, meta and para situations

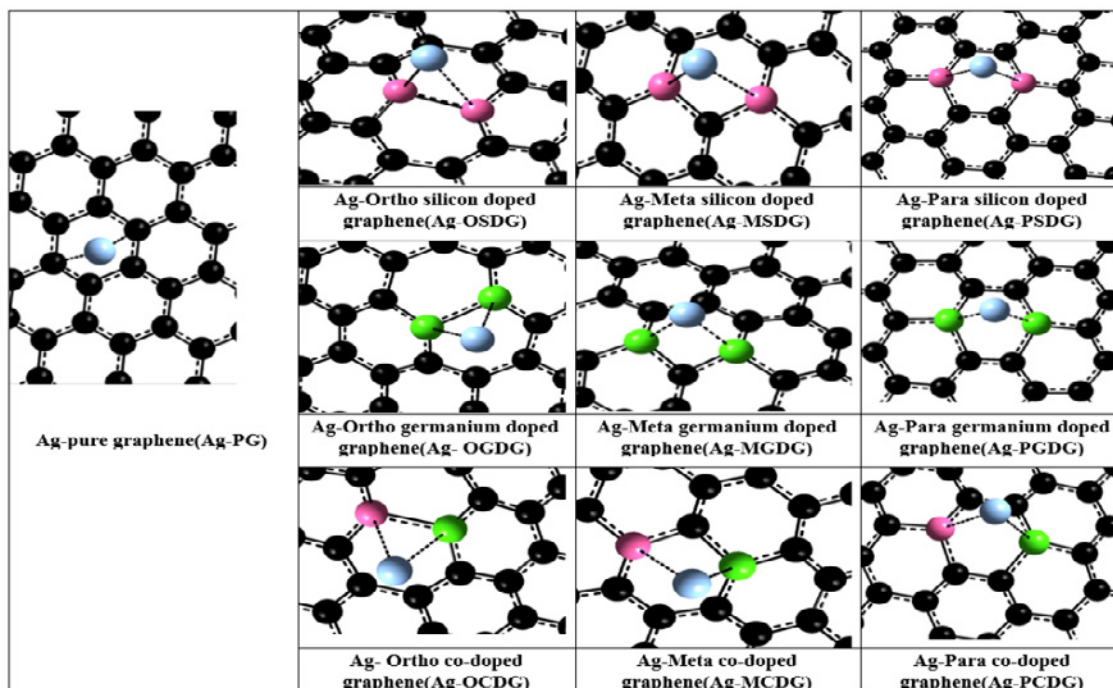


Fig. 3. The optimized structures of the derived complexes of silver with various nano adsorbents and their abbreviated names
Atom colors: black—carbon, green—germanium, pink—silicon, and blue—silver

numbered with one and two consecutively in order to report the bond lengths more easily. The ortho silicon doped graphene is symbolized by OSDG and its derivative with silver is defined as Ag-OSDG. The meta silicon doped graphene is remarked by MSDG abbreviation and Ag-MSDG is specified for its derived product with silver. The PSDG and Ag-PSDG signs were assigned for para silicon doped graphene and its complex with Ag⁺ respectively.

In the third step, the graphene was doped with germanium at three ortho, meta and para positions. The OGDG and Ag-OGDG were heeded as symbols for ortho germanium doped graphene and Ag-ortho germanium doped graphene respectively. The meta germanium doped graphene was abbreviated as MGDG and its derived complex with Ag⁺ is exhibited by Ag-MGDG sign. The PGDG and Ag-PGDG symbols were also considered for para germanium doped graphene and Ag-para germanium doped graphene.

In the end, the nano-adsorbent was doped with one silicon and one germanium elements in ortho, meta and para situations. The ortho co-doped graphene and its silver derivative were remarked as OCDG and Ag-OCDG respectively. MCDG and Ag-MCDG stand for meta co-doped graphene and its silver derived product. PCDG was allocated for para co-doped graphene and Ag-PCDG was determined for the derived product of silver and para co-doped graphene interaction.

Adsorption Energy Values

In order to achieve adsorption energies of silver (I) on the surface of the 10 nano adsorbents, geometrical optimizations were implemented on the structures of Ag⁺, ordinary and doped graphenes and their derivatives. Then adsorption energy values were calculated by the succeeding equation:

$$E_{\text{ads}} = E_{\text{Ag-adsorbent}} - (E_{\text{Ag}} + E_{\text{adsorbent}}) \quad (1)$$

Afterward, the obtained results were reported in Table 1. As the provided data in the table reveals clearly the adsorption energy of the pure graphene (-477.03 KJ/mol) is more positive than the other doped graphenes. Indeed, by superseding two carbon atoms with silicon and germanium, the adsorption process has become more experimentally feasible. In the case of silicon doped graphenes, Ag-OSDG has the lowest adsorption energy (-814.911 KJ/mol) but by increasing the distance of the dopant atoms, this parameter has become more positive gradually so that PSDG has the most positive adsorption energy among the silicon-doped graphenes (-669.450 KJ/mol). On the other hand, in the case of germanium doped nano-adsorbents, there is not seen any regular trend. We cannot find an obvious relationship between the adsorption energy and the distance of the germanium atoms. Because E_{ads} has decreased from -774.667 KJ/mol in the ortho situation to the -901.534 KJ/mol in the meta position. But by enhancing the distance of the germanium atoms in the para condition this variable has risen significantly to -605.590 KJ/mol. Nevertheless, it seems ortho co-doped graphene which is entailed of one silicon and one germanium elements has the best interaction with silver owing to its lowest adsorption energy (-1143.038 KJ/mol). The next matter that can be perceived from the table is that co-doped graphenes exhibit a similar trend towards Ag⁺, to Si-doped graphenes. In other words, by incrementing the distance between the dopant atoms, E_{ads} experience a dramatic surge from the -1143.038 KJ/mol in ortho position to -560.783 KJ/mol at para condition [28].

It is worth mentioning that according to the carried out calculations there was not observed

Table 1. Adsorption energy values, lowest frequency and bond lengths for the Ag⁺ adsorption process

Derived complexes	The total electronic energy of Ag ⁺ (KJ/mol)	The total electronic energy of adsorbents (KJ/mol)	The total electronic energy of the derived products (KJ/mol)	E_{ads} (KJ/mol)	Lowest frequency (cm ⁻¹)	M-Ge ₁ (Å)	M-Ge ₂ (Å)	M-Si ₁ (Å)	M-Si ₂ (Å)	M-C ₁ (Å)	M-C ₂ (Å)
Ag-PG	-13511442.2	-3139680.8	-16651600	-477.03	49.328					1.763	2.293
Ag-OSDG	-13511442.2	-4442246.23	-17954503.3	-814.91	43.166			2.172	3.889		
Ag-MSDG	-13511442.2	-4442593.42	-17954783.1	-747.46	53.748			2.309	4.246		
Ag-PSDG	-13511442.2	-4442683.11	-17954794.7	-669.45	62.629			2.389	3.432		
Ag-OGDG	-13511442.2	-13716404.6	-27228621.4	-774.67	54.976	2.213	2.213				
Ag-MGDG	-13511442.2	-13716718.2	-27229062	-901.53	54.398	2.266	2.331				
Ag-PGDG	-13511442.2	-13716808.8	-27228856.5	-605.59	51.669	2.185	2.154				
Ag-OCDG	-13511442.2	-9079316	-22591901.1	-1143	57.395	2.295			4.443		
Ag-MCDG	-13511442.2	-9079665.88	-22591775.5	-667.48	47.089	2.343			3.049		
Ag-PCDG	-13511442.2	-9079748.35	-22591751.3	-560.78	52.212	2.163			2.156		

any negative frequency in all of the investigated structures. The lowest frequency for all of the derivatives is also reported in Table 1.

Calculation and Verifying the Values of Enthalpy Changes (ΔH_{ad})

In order to obtain enthalpy alterations, the thermal enthalpy values for the reactants and products of the adsorption process that had been computed by the software were inserted in the following formula:

$$\Delta H_{ad} = \Delta E^* + (H_{th(Ag-adsorbent)} - (H_{th(silver)} + H_{th(adsorbent)})) \quad (2)$$

In the aforementioned equation, ΔE^* stands for the variations in the total energy of the desired procedure. As the provided data in Table 2, demonstrates obviously, ΔH_{ad} has fallen significantly after doping graphene with two other elements. In fact, adsorption of Ag^+ on the surface of the doped nano-adsorbents is more exothermic than its adsorption on the pure graphene. Among Si-doped graphenes, OSDG has the lowest ΔH_{ad} value (-812.085 KJ/mol in the room temperature) but by increasing the distance of the dopant elements in meta and para positions, this parameter has got more positive. This pattern is also observed in co-doped graphenes. As it can be witnessed from the table, Ag-OCDG has the most negative (-1131.077 KJ/mol) among all of the studied derivatives. It

means silver can be absorbed by the ortho co-doped graphene more exothermically than the other ones. However, the enthalpy changes values of Ag-MCDG and Ag-PCDG is substantially more positive than Ag-OCDG. In the case of germanium doped graphenes, the ΔH_{ad} does not show any dependence to the situations and closeness of the germanium atoms because enthalpy alterations value has decreased from -774.001 KJ/mol Ag-OGDG to -889.653 KJ/mol. On the other hand, this variable has reduced again to -608.565 KJ/mol in Ag-PGDG derivative.

For evaluating the impression of temperature on the adsorption process of the silver ions the IR calculations were implemented in the temperature range of 298.15-398.25 K at 10-degree intervals. As it is apparent from the table in all derivatives ΔH_{ad} experiences a modest and negligible rise by gradual enhancing the temperature. So generally, temperature variations do not have a tangible impact on the enthalpy changes.

Calculation and Verifying the Values of Gibbs Free Energy Changes (ΔG_{ad}) and Thermodynamic Constant (K_{th})

For calculating Gibbs free energy changes for the adsorption process the subsequent equation would be utilized:

$$\Delta G_{ad} = \Delta E^* + [G_{th(Ag-adsorbent)}] - [G_{th(Silver)} + G_{th(Adsorbent)}] \quad (3)$$

Table 2. Enthalpy changes values for the adsorption of silver (I) on the surface of ordinary and doped graphenes in the temperature range of 300-400 K.

ΔH_{ad} (KJ/mol)					
Temperature (K)	Ag-PG	Ag-OSDG	Ag-MSDG	Ag-PSDG	Ag-OGDG
298.15	-477.952	-812.085	-741.780	-669.282	-774.001
308.15	-477.849	-811.864	-741.631	-669.132	-773.771
318.15	-477.745	-811.646	-741.472	-669.007	-773.571
328.15	-477.639	-811.429	-741.318	-668.902	-773.417
338.15	-477.533	-811.266	-741.165	-668.775	-773.294
348.15	-477.426	-811.091	-740.980	-668.632	-773.154
358.15	-477.317	-810.927	-740.781	-668.480	-773.026
368.15	-477.189	-810.761	-740.582	-668.313	-772.94
378.15	-477.031	-810.608	-740.417	-668.168	-772.836
388.15	-476.926	-810.431	-740.275	-668.014	-772.681
398.15	-476.812	-810.250	-740.136	-667.859	-772.506
Temperature (K)	Ag-MGDG	Ag-PGDG	Ag-OCDG	Ag-MCDG	Ag-PCDG
298.15	-889.653	-608.565	-1131.077	-665.268	-564.395
308.15	-889.518	-608.372	-1130.893	-665.098	-564.207
318.15	-889.381	-608.201	-1130.726	-664.960	-564.039
328.15	-889.241	-608.001	-1130.588	-664.814	-563.878
338.15	-889.085	-607.804	-1130.472	-664.667	-563.711
348.15	-888.929	-607.610	-1130.340	-664.516	-563.526
358.15	-888.813	-607.420	-1130.229	-664.364	-563.336
368.15	-888.715	-607.256	-1130.151	-664.237	-563.162
378.15	-888.614	-607.121	-1130.074	-664.117	-562.996
388.15	-888.516	-606.942	-1130.002	-664.018	-562.836
398.15	-888.407	-606.784	-1129.929	-663.898	-562.675

In this formula, G_{th} is thermal Gibbs free energy for the reactants and the products of the interaction between the heavy metal and nano-adsorbents and ΔE° is the alterations in the total energy of the system. As the reported ΔG_{ad} values in Table 3 exhibit obviously, the Gibbs free energy alterations for the adsorption of Ag^+ on the ordinary graphene is more positive than the doped graphenes which imply that silver can be absorbed by the doped graphenes more spontaneously. The achieved ΔG_{ad} values are in good agreement with the previously obtained adsorption energies and enthalpy changes. Ag-OCDG has the most negative Gibbs free energy alteration values with a great discrepancy. In silicon doped graphenes Ag-OSDG has lower ΔG_{ad} than Ag-MSDG and Ag-OGDG. In the case of germanium doped graphenes, the most negative ΔG_{ad} is seen at meta position (-847.404 KJ/mol at ambient temperature) and this parameter is more positive for para and ortho situations due to their higher ΔG_{ad} . It seems the increasing of the temperature cause a slight decline in the Gibbs free energy values. Indeed, the temperature variations do not cause a remarkable change in this variable [28-30].

The thermodynamic equilibrium constants were also calculated for the desired adsorption process by using equation 4 and the achieved results were tabulated in Table 4. As it can be observed, the results are not out of expecting

and ortho co-doped graphene shows the greatest thermodynamic equilibrium constant which is another proof that substantiates OCDG is the best adsorbent for silver cations. But the hidden point is that K_{th} has reduced tangibly by enhancing temperature. This phenomenon implies that the optimum temperature for the adsorption process is 298.15 K. Despite the fact that we observed a decline in the ΔG_{ad} values for all derivatives by incrementing the temperature in the prior table but those alterations were not meaningful. In addition, owing to the fact that the temperature which is located in the denominator of equation 4 has changed more severely in comparison to ΔG_{ad} , it shows its influence more sharply. Therefore, the thermodynamic equilibrium constant has decreased at higher temperatures. Hence, it can be deduced that 298.15 is the best temperature for the investigated procedure.

$$K = \exp(-\Delta G_{ad}/RT) \quad (4)$$

Calculation and Inquiring the Specific Heat Capacity (C_v)

The Specific heat capacity values of the silver, adsorbents and the derived product from the interaction between the heavy metal and pure and doped graphenes were computed by Spartan software and the obtained values were presented in Table 5. As it can be witnessed from the table,

Table 3. Gibbs free energy changes values for the adsorption of silver (I) on the surface of ordinary and doped graphenes in the temperature range of 300-400 K.

Temperature (K)	ΔG_{ad} (KJ/mol)				
	Ag-PG	Ag-OSDG	Ag-MSDG	Ag-PSDG	Ag-OGDG
298.15	-436.651	-773.557	-700.477	-624.978	-734.305
308.15	-436.967	-773.905	-700.825	-625.161	-734.623
318.15	-437.285	-774.187	-701.128	-625.448	-735.04
328.15	-437.605	-774.475	-701.376	-625.695	-735.498
338.15	-437.927	-774.887	-701.569	-625.913	-735.99
348.15	-438.181	-775.261	-701.727	-626.118	-736.507
358.15	-438.469	-775.650	-701.868	-626.316	-737.081
368.15	-438.698	-776.116	-702.006	-626.503	-737.656
378.15	-438.898	-776.584	-702.224	-626.674	-738.181
388.15	-439.151	-777.067	-702.457	-626.799	-738.533
398.15	-439.399	-777.474	-702.648	-626.857	-738.811
Temperature (K)	Ag-MGDG	Ag-PGDG	Ag-OCDG	Ag-MCDG	Ag-PCDG
298.15	-847.404	-565.299	-1088.473	-620.866	-520.989
308.15	-847.657	-565.537	-1088.648	-621.103	-521.254
318.15	-847.875	-565.721	-1088.838	-621.377	-521.495
328.15	-848.058	-565.859	-1089.028	-621.574	-521.748
338.15	-848.239	-566.001	-1089.266	-621.770	-521.999
348.15	-848.414	-566.206	-1089.530	-621.940	-522.235
358.15	-848.581	-566.444	-1089.928	-622.195	-522.396
368.15	-848.784	-566.721	-1090.362	-622.483	-522.639
378.15	-849.003	-566.993	-1090.794	-622.717	-522.877
388.15	-849.238	-567.196	-1091.166	-622.928	-523.077
398.15	-849.461	-567.529	-1091.476	-623.159	-523.278

Table 4. Thermodynamic equilibrium constants for the adsorption of silver (I) on the surface of ordinary and doped graphenes in the temperature range of 300-400 K.

Temperature (K)	K_{th}				
	Ag-PG	Ag-OSDG	Ag-MSDG	Ag-PSDG	Ag-OGDG
298.15	3.178×10^{-76}	$3.379 \times 10^{+135}$	5.309×10^{-122}	$3.144 \times 10^{+109}$	4.486×10^{-128}
308.15	1.183×10^{-74}	$1.548 \times 10^{+131}$	$6.331 \times 10^{+118}$	$9.442 \times 10^{+105}$	3.395×10^{-124}
318.15	6.267×10^{-71}	$1.295 \times 10^{+127}$	$1.309 \times 10^{+115}$	$4.912 \times 10^{+102}$	4.842×10^{-120}
328.15	4.572×10^{-69}	$1.926 \times 10^{+123}$	$4.452 \times 10^{+111}$	$3.991 \times 10^{+99}$	1.203×10^{-117}
338.15	4.466×10^{-67}	$5.040 \times 10^{+119}$	$2.380 \times 10^{+108}$	$4.890 \times 10^{+96}$	4.941×10^{-113}
348.15	5.557×10^{-65}	$2.091 \times 10^{+116}$	$1.938 \times 10^{+105}$	$8.767 \times 10^{+93}$	3.205×10^{-110}
358.15	8.935×10^{-63}	$1.347 \times 10^{+113}$	$2.334 \times 10^{+102}$	$2.233 \times 10^{+91}$	3.192×10^{-107}
368.15	1.764×10^{-62}	$1.326 \times 10^{+110}$	$4.047 \times 10^{+99}$	$7.834 \times 10^{+88}$	4.629×10^{-104}
378.15	4.247×10^{-60}	$1.884 \times 10^{+107}$	$1.007 \times 10^{+97}$	$3.689 \times 10^{+86}$	9.335×10^{-101}
388.15	1.259×10^{-59}	$3.769 \times 10^{+104}$	$3.431 \times 10^{+94}$	$2.257 \times 10^{+84}$	2.457×10^{-99}
398.15	4.449×10^{-57}	$1.007 \times 10^{+102}$	$1.535 \times 10^{+92}$	$1.748 \times 10^{+82}$	8.523×10^{-96}
Temperature (K)	Ag-MGDG	Ag-PGDG	Ag-OCDG	Ag-MCDG	Ag-PCDG
298.15	$2.931 \times 10^{+148}$	$1.101 \times 10^{+99}$	5.044×10^{-190}	$5.986 \times 10^{+108}$	1.899×10^{-91}
308.15	$4.919 \times 10^{+143}$	$7.377 \times 10^{+95}$	$3.498 \times 10^{+184}$	$1.937 \times 10^{+105}$	2.297×10^{-88}
318.15	$1.627 \times 10^{+139}$	$7.671 \times 10^{+92}$	$5.950 \times 10^{+178}$	$1.054 \times 10^{+102}$	4.201×10^{-85}
328.15	$9.956 \times 10^{+134}$	$1.192 \times 10^{+90}$	$2.274 \times 10^{+173}$	$8.814 \times 10^{+98}$	1.134×10^{-83}
338.15	$1.081 \times 10^{+131}$	$2.719 \times 10^{+87}$	$1.849 \times 10^{+168}$	$1.120 \times 10^{+96}$	4.335×10^{-80}
348.15	$1.978 \times 10^{+127}$	$8.989 \times 10^{+84}$	$2.974 \times 10^{+163}$	$2.070 \times 10^{+93}$	2.272×10^{-78}
358.15	$5.838 \times 10^{+123}$	$4.135 \times 10^{+82}$	$9.269 \times 10^{+158}$	$5.595 \times 10^{+90}$	1.556×10^{-76}
368.15	$2.712 \times 10^{+120}$	$2.580 \times 10^{+80}$	$5.137 \times 10^{+154}$	$2.107 \times 10^{+88}$	1.435×10^{-74}
378.15	$1.900 \times 10^{+117}$	$2.102 \times 10^{+78}$	$4.776 \times 10^{+150}$	$1.048 \times 10^{+86}$	1.693×10^{-72}
388.15	$1.945 \times 10^{+114}$	$2.149 \times 10^{+76}$	$7.033 \times 10^{+146}$	$6.800 \times 10^{+83}$	2.482×10^{-70}
398.15	$2.803 \times 10^{+111}$	$2.876 \times 10^{+74}$	$1.584 \times 10^{+143}$	$5.719 \times 10^{+81}$	4.498×10^{-68}

Table 5. The specific heat capacity of the investigated materials in this study

Temperature (K)	C_v (J/mol .K)						
	Ag ⁺	PG	Ag-PG	OSDG	Ag-OSDG	MSDG	Ag-MSDG
298.15	12.472	303.479	325.119	325.780	353.765	324.410	353.614
	PSDG	Ag-PSDG	OGDG	Ag-OGDG	MGDG	Ag-MGDG	PGDG
	322.525	345.337	335.614	362.425	335.522	361.386	333.665
	Ag-PGDG	OCDG	Ag-OCDG	MCDG	Ag-MCDG	PCDG	Ag-PCDG
	360.423	330.738	350.074	329.672	352.218	328.194	354.727

there is a considerable gap between the C_v of the cation and evaluated nano-adsorbents, and after the adsorption of Ag⁺, a remarkable increase has taken place in the specific heat capacity of the investigated nanostructures. For example, in the case of pure graphene, the C_v of Ag⁺ in the ambient temperature is 12.472 J/mol. K and the specific heat capacity for graphene are 303.479 J/mol.K but after the junction of silver on the surface of the graphene, this factor has risen to the value of 325.119 J/mol.K. This phenomenon can be seen in all of the situations. Due to the fact that C_v has a linear and direct relationship with the thermal conductivity according to equation 5. Hence, it can be inferred the thermal conductivity of the ordinary and doped graphenes could be ameliorated after binding to silver ions. This phenomenon is worthwhile because, in the construction and development of thermal sensors, a meaningful variation in thermal conductivity is of great importance. Moreover, our

prior studies in the ΔH_{ad} values proved that the adsorption procedure of Ag⁺ on all of the studied structures is exothermic and in other words, heat and energy are produced in this process and transferred from the system to the environment. Thus, production of heat and also defusing of specific heat capacity and thermal conductivity are valuable evidence which reveals that pure and doped graphenes can be eminent sensing materials for designing a silver (I) thermal sensor [38].

$$K = \frac{n \langle v \rangle \lambda C_v}{3N} \quad (5)$$

In the fifth equation, K, n, $\langle v \rangle$, λ , C_v and N are thermal conductivity, particles per unit, mean particle speed, mean free path, molecular specific heat capacity, and Avogadro's number respectively. Fig. 4 depicts the influence of changing the temperature on the heat capacity of the ordinary

and doped graphenes. As it is obvious from the diagram, by incrementing the temperature this parameter has also increased linearly. But with a closer look, it can be perceived that there is not a remarkable discrepancy between the pure graphene and the doped ones. In fact, all curves have a similar slope to each other and the only difference that can be witnessed among them is the negligible alterations in the intercept.

Frontier Molecular Orbital Analysis

Some Structural features including energies of HOMO and LUMO molecular orbitals (E_H , E_L), distance between energies of HOMO and LUMO molecular orbitals (HLG), electrophilicity (ω),

dipole moment, maximum transmitted electron (ΔN_{max}) and chemical hardness (η) were also evaluated. HOMO and LUMO are the highest occupied molecular orbital and the lowest unoccupied molecular orbital respectively. And the energy difference between them is known as the HOMO–LUMO gap or energy gap (HLG) which could be calculated from equation 6. As it can be observed from the calculated energy gap values in Table 6 and also density of states (DOS) plots in Figs. 5 and 6, this parameter has increased after the adsorption of silver on the surface of all of the nano-adsorbents except in the case of pure graphene, PGDG, and MCDG. And owing to the fact a higher energy gap value of a compound

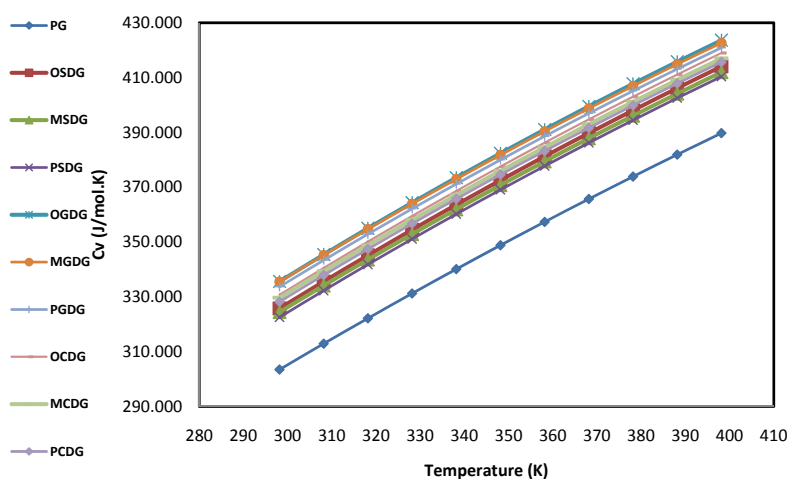


Fig. 4. The specific heat capacity of the nano-adsorbents in the temperature range of 298.15 to 398.15 K at 10° intervals.

Table 6. Calculated E_H and E_L , HLG, chemical hardness (η), electrophilicity index (ω), and the maximum amount of electronic charge index, ΔN_{max} and dipole moment for the silver adsorption process

	E_H (eV)	E_L (eV)	HLG (eV)	η (eV)	ω (eV)	ΔN_{max} (eV)	Dipole moment (deby)
Ag	-9.2	-3.11	6.09	3.045	6.221	2.021	0
PG	-6.94	0.66	7.60	3.800	1.297	0.826	0
Ag-PG	-9.79	-2.64	7.15	3.575	5.402	1.738	5.31
OSDG	-4.9	1.29	6.19	3.095	0.526	0.583	0
Ag- OSDG	-9.49	-1.75	7.74	3.870	4.081	1.452	6.8
MSDG	-5.58	1.13	6.71	3.355	0.738	0.663	3.86
Ag- MSDG	-8.57	-1.64	6.93	3.465	3.761	1.473	8.58
PSDG	-5.44	0.93	6.37	3.185	0.798	0.708	3.43
Ag- PSDG	-9.32	-2.07	7.25	3.625	4.474	1.571	6.49
OGDG	-5.3	1.18	6.48	3.240	0.655	0.636	0
Ag- OGDG	-9.21	-2.68	6.53	3.265	5.412	1.821	7.09
MGDG	-5.83	1.07	6.90	3.450	0.821	0.690	3.01
Ag- MGDG	-8.96	-1.43	7.53	3.765	3.584	1.380	7.46
PGDG	-5.76	0.93	6.69	3.345	0.872	0.722	2.51
Ag- PGDG	-9.55	-2.91	6.64	3.320	5.845	1.877	5.72
OCDG	-5.11	1.23	6.34	3.170	0.594	0.612	0.93
Ag-OCDG	-9.39	-1.88	7.51	3.755	4.228	1.501	5.25
MCDG	-5.76	1.13	6.89	3.445	0.778	0.672	3.16
Ag-MCDG	-9.02	-2.2	6.82	3.410	4.615	1.645	6.48
PCDG	-5.61	0.92	6.53	3.265	0.842	0.718	2.52
Ag- PCDG	-9.58	-2.92	6.66	3.330	5.865	1.877	6.46

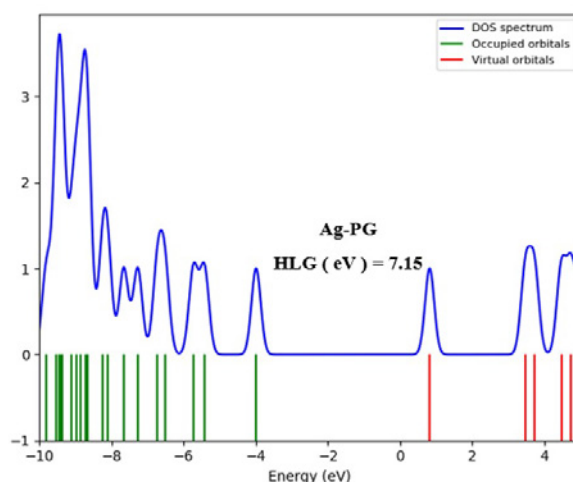


Fig. 5. DOS diagram of Ag-PG

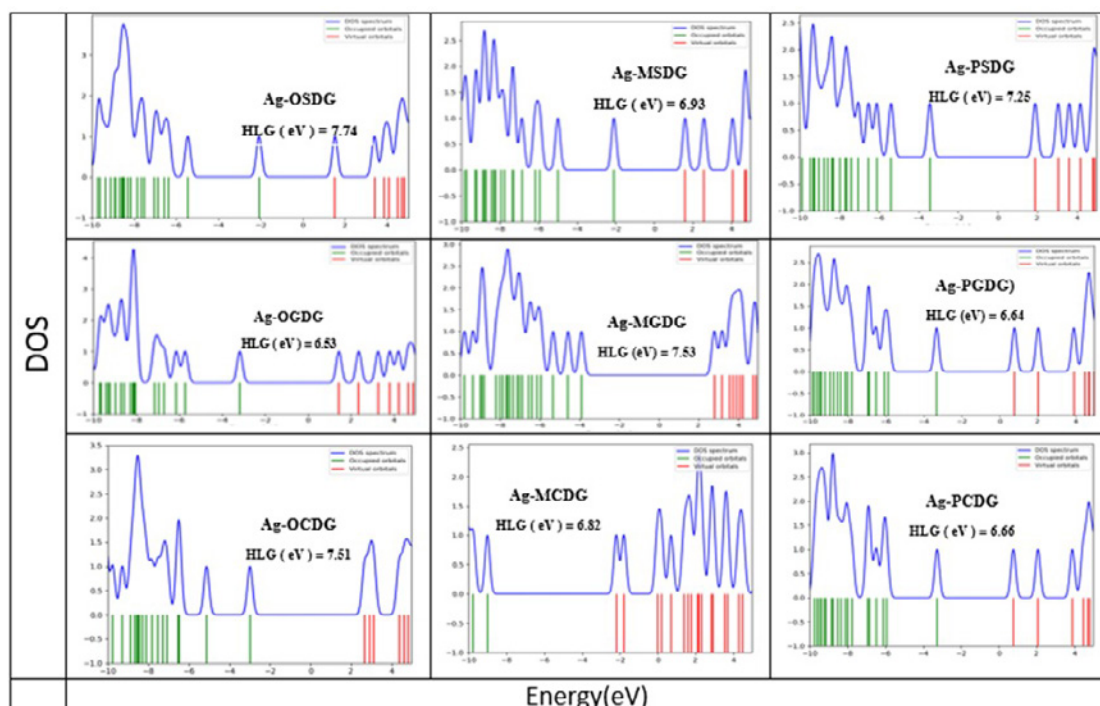


Fig. 6. DOS diagrams of the Silver(I) and doped graphenes derived products

exhibits that more excitation energy is required for conveying the electron to the excited state. Hence, it can be elicited that the conductivity of Ag^+ and adsorbents has declined after the junction of the heavy metal in most cases except pure graphene, PGDG, and MCDG. The next matter that can be realized from the HLG values is that this variable is about 6-7.5 (eV) in all cases and has not experienced a significant alteration at all. In fact, all of the investigated structures are non-conductor

and because the electrochemical conductometric analytical methods are designed on the basis of substantial variations in the electrochemical conductance of a system or reaction. Therefore, ordinary and doped graphene cannot be an appropriate material in the development of conductometric sensors for determination of Ag^+ .

Chemical hardness is the next investigated parameter which was calculated via equation 7. Chemical hardness is an excellent variable for

estimating the softness of material. Indeed, a substance with a large HOMO-LUMO gap is harder than a compound with a small HOMO-LUMO gap. By a closer look at Table 6, it can be understood that graphene's chemical hardness has reduced after doping it with silicon and germanium. Due to the fact that soft compounds can change their electron density more easily than hard materials. Hence, doped graphenes are more reactive than ordinary graphene. Because transmission of electrons which is necessary for the implementation of chemical reactions can be done more conveniently in the doped graphenes. After the attachment of silver ion on adsorbents, chemical hardness has incremented in all situations except pure graphene, PGDG, and MCDG.

Electrophilicity index (ω) is an admissible criterion for estimating the tendency of a molecule towards electron. This index was calculated via equation 8. While two molecules take part in a reaction, one of them behaves like a nucleophile, whereas the other one plays the role of an electrophile. A great electrophilicity value for a substance substantiates that the molecule has high electrophilic power. Thus, the quantity of ω describes the propensity of the system to acquire an additional electronic charge from the environment. The maximum amount of electronic charge index (ΔN_{\max}) which was obtained by using equation 9, reveals the charge capacity of a system. In other words, a compound with a positive value of ΔN_{\max} index acts as an electron acceptor, whilst a molecule with a negative value of ΔN_{\max} index acts as an electron donor. As it can be seen from the provided data in the table, the cation has the most positive electrophilicity index and ΔN_{\max} (6.221 and 2.021 (eV) respectively) among all of the studied structures which shows that this cation behaves like a strong Lewis acid. But on the other hand, these parameters are lower for all of the nano-adsorbents with a tangible difference. therefore, it can be estimated that they can act the role of Lewis base or a ligand. By comparing the pure graphene and the doped ones it can be perceived that doping graphene with germanium and silicon leads to remarkable abate in both ω and ΔN_{\max} parameters. In fact, the affinity of the graphene to electron has decreased after the doping process. In other words, the doped graphenes can be a stronger Lewis base or ligand than the ordinary graphene. Hence, the toxic cation and doped graphenes with silicon and germanium can undergo the complexation

reaction and this fact implies that doped graphenes could act as a prominent neutral ion carrier in the construction of potentiometric ion-selective electrodes for determination of Ag^+ . Another valuable point that is obvious from the table is that both of the ω and ΔN_{\max} variables have incremented after the junction of the silver ion on the surface of the adsorbents in all cases. So, the adsorbent has become more electrophile after the adsorption procedure [24].

$$\text{HLG} = E_{\text{LUMO}} - E_{\text{HOMO}} \quad (6)$$

$$\eta = (E_{\text{LUMO}} - E_{\text{HOMO}})/2 \quad (7)$$

$$\omega = \mu^2/2\eta \quad (8)$$

$$\Delta N_{\max} = -\mu/\eta \quad (9)$$

The dipole moment is a good standard for inspecting the solubility of a compound because it has a direct relationship with solubility. Indeed, structures with higher dipole moment values have better solubility in polar solvents like water. The achieved results from the calculation in the table show that the dipole moment has enhanced after the binding of silver to the adsorbents. Therefore, the solubility and reactivity of the system have improved after the junction. It is worth mentioning that in both removals of heavy metals and also sensor subjects, the low solubility of the adsorbent is of great importance. In this regards, it seems pure graphene, OSDG, OGDG, and OCDG structures are superior to other adsorbents in terms of low solubility owing to their negligible dipole moment values.

CONCLUSIONS

Silver is a toxic heavy metal that is widely utilized in various industries. Hence, it can be a potential contaminant for the environment. In addition, high dosages of Ag^+ can cause severe and irreversible damages for all of the living organisms. Therefore, its removal and determination are very important. In this regard, the adsorption of Silver (I) cations on the surface of graphene and the influence of doping graphene with silicon and germanium on this process were investigated in this study at ten configurations. The achieved results show that ortho co-doped graphene has the best and the strongest interaction with Ag^+ because it has the lowest adsorption energy, enthalpy changes, and

Gibbs free energy alterations values among all of the evaluated adsorbents. The impact of temperature on the adsorption procedure was also studied and the obtained results reveal that the ambient temperature is the best and optimum temperature for all of the studied configurations. The calculated specific heat capacity values for all of the situations demonstrate that the thermal conductivity of all of the adsorbents has increased dramatically after the junction of the cation on the surface of the pure and doped graphenes. So, graphene could be a superb sensing material for construction of thermal sensors. Owing to the fact that energy gap values of all of the studied structures were considerably high, it seems ordinary and doped graphenes cannot be an appropriate electroactive sensing material in the development of conductometric sensors. But the obtained electrophilicity values exhibit that silver and all of the adsorbents can undergo complexation reaction. Thus, using pure and doped graphenes in the development of potentiometric ion-selective electrodes seems logical. Owing to the fact that the achieved results in this research prove the ortho silicon doped graphene has a strong interaction with Ag^+ , the capability of this nanostructure in the removal and determination of Silver (I) cations had better be investigated experimentally by the experts of this field.

CONFLICT OF INTEREST

The authors declare that there are no conflicts of interest regarding the publication of this manuscript.

REFERENCES

- Zhang Y, Chen W, Dong X, Fan H, Wang X, Bian L. Simultaneous detection of trace toxic metal ions, Pb^{2+} and Ag^+ , in water and food using a novel single-labeled fluorescent oligonucleotide probe. *Sensors and Actuators B: Chemical*. 2018;261:58-65.
- Yan Z, Lu Y, Wang H, Wu S, Zhao B. A heterocycle functionalized p-tert-butylcalix[4]arene as a neutral carrier for silver (I) ion-selective electrode. *Journal of Molecular Liquids*. 2013;183:72-8.
- Wu H, Jia J, Xu Y, Qian X, Zhu W. A reusable bifunctional fluorescent sensor for the detection and removal of silver ions in aqueous solutions. *Sensors and Actuators B: Chemical*. 2018;265:59-66.
- Sarı A, Tüzen M. Adsorption of silver from aqueous solution onto raw vermiculite and manganese oxide-modified vermiculite. *Microporous and Mesoporous Materials*. 2013;170:155-63.
- Said NR, Rezayi M, Narimani L, Al-Mohammed NN, Manan NSA, Alias Y. A New N-Heterocyclic Carbene Ionophore in Plasticizer-free Polypyrrole Membrane for Determining Ag^+ in Tap Water. *Electrochimica Acta*. 2016;197:10-22.
- Pourreza N, Rastegarzadeh S, Larki A. Nano-TiO₂ modified with 2-mercaptobenzimidazole as an efficient adsorbent for removal of $\text{Ag}(\text{I})$ from aqueous solutions. *Journal of Industrial and Engineering Chemistry*. 2014;20(1):127-32.
- Nitayaphat W, Jintakosol T. Removal of silver(I) from aqueous solutions by chitosan/bamboo charcoal composite beads. *Journal of Cleaner Production*. 2015;87:850-5.
- Evtugyn GA, Stoikov II, Beljyakova SV, Shamagsumova RV, Stoikova EE, Zhukov AY, et al. Ag^+ selective electrode based on glassy carbon electrode covered with polyaniline and thiacalix[4]arene as neutral carrier. *Talanta*. 2007;71(4):1720-7.
- Elwakeel KZ, El-Sayed GO, Darweesh RS. Fast and selective removal of silver(I) from aqueous media by modified chitosan resins. *International Journal of Mineral Processing*. 2013;120:26-34.
- Akgül M, Karabakan A, Acar O, Yürüm Y. Removal of silver (I) from aqueous solutions with clinoptilolite. *Microporous and Mesoporous Materials*. 2006;94(1-3):99-104.
- Karimi Raja, M. K. and R. Ahmadi, 2015. Investigation of Adsorption Enthalpy of Prolin on the Surface of Graphene with and without Si: A DFT Study. *International Journal of New Chemistry*, 2(3): 223-227.
- Hassani A, Mosavian MTH, Ahmadpour A, Farhadian N. A comparative theoretical study of methane adsorption on the nitrogen, boron and lithium doped graphene sheets including density functional dispersion correction. *Computational and Theoretical Chemistry*. 2016;1084:43-50.
- Zhang H-p, Luo X-g, Lin X-y, Lu X, Leng Y, Song H-t. Density functional theory calculations on the adsorption of formaldehyde and other harmful gases on pure, Ti-doped, or N-doped graphene sheets. *Applied Surface Science*. 2013;283:559-65.
- Shokuhi Rad A, Sani E, Binaeian E, Peyravi M, Jahanshahi M. DFT study on the adsorption of diethyl, ethyl methyl, and dimethyl ethers on the surface of gallium doped graphene. *Applied Surface Science*. 2017;401:156-61.
- Li L, Gong L, Wang Y-X, Liu Q, Zhang J, Mu Y, et al. Removal of halogenated emerging contaminants from water by nitrogen-doped graphene decorated with palladium nanoparticles: Experimental investigation and theoretical analysis. *Water Research*. 2016;98:235-41.
- Wanno B, Tabtimsai C. A DFT investigation of CO adsorption on VIII B transition metal-doped graphene sheets. *Superlattices and Microstructures*. 2014;67:110-7.
- Liang X-Y, Ding N, Ng S-P, Wu C-ML. Adsorption of gas molecules on Ga-doped graphene and effect of applied electric field: A DFT study. *Applied Surface Science*. 2017;411:11-7.
- Shokuhi Rad A. Adsorption of mercaptopyridine on the surface of Al- and B-doped graphenes: Theoretical study. *Journal of Alloys and Compounds*. 2016;682:345-51.
- Cortés-Arriagada D, Villegas-Escobar N. A DFT analysis of the adsorption of nitrogen oxides on Fe-doped graphene, and the electric field induced desorption. *Applied Surface Science*. 2017;420:446-55.
- Cortés-Arriagada D, Villegas-Escobar N, Ortega DE. Fe-doped graphene nanosheet as an adsorption platform of harmful gas molecules (CO , CO_2 , SO_2 and H_2S), and

- the co-adsorption in O₂ environments. *Applied Surface Science*. 2018;427:227-36.
21. Bakhshi F, Farhadian N. Co-doped graphene sheets as a novel adsorbent for hydrogen storage: DFT and DFT-D3 correction dispersion study. *International Journal of Hydrogen Energy*. 2018;43(17):8355-64.
 22. Farmanzadeh D, Abdollahi T. H₂ adsorption on free and graphene-supported Ni nanoclusters: A theoretical study. *Surface Science*. 2018;668:85-92.
 23. Özkaya S, Blaisten-Barojas E. Polypyrrole on graphene: A density functional theory study. *Surface Science*. 2018;674:1-5.
 24. Luo D, Zhang X. The effect of oxygen-containing functional groups on the H₂ adsorption of graphene-based nanomaterials: experiment and theory. *International Journal of Hydrogen Energy*. 2018;43(11):5668-79.
 25. Esrafil MD, Dinparast L. The selective adsorption of formaldehyde and methanol over Al- or Si-decorated graphene oxide: A DFT study. *Journal of Molecular Graphics and Modelling*. 2018;80:25-31.
 26. Janani K, John Thiruvadigal D. Adsorption of essential minerals on l-glutamine functionalized zigzag graphene nanoribbon-A first principles DFT study. *Applied Surface Science*. 2018;449:829-37.
 27. Ahmadi, R., and M. R. Jalali Sarvestani, 2018. Investigating the Effect of Doping Graphene with Silicon in the Adsorption of Alanine by Density Functional Theory. *Physical Chemistry Research*, 6(3): 639-655.
 28. Ahmadi, R., and M. R. Jalali Sarvestani, 2018. Computational investigation of the influence of carbon nanostructures on the properties of energetic TATB substance by DFT method. *International Journal of Bio-Inorganic Hybrid Nanomaterials*, 6 (4): 239-244.
 29. Ahmadi R, Soleymani R. The Influence of Tyrozine on Energetic Property in Graphene Oxide: A DFT Study. *Oriental Journal of Chemistry*. 2014;30(1):57-62.
 30. Ahmadi, R., and M. Pirahan Foroush, 2014. Fullerene effect on chemical properties of antihypertensive clonidine in water phase. *Annals of Military and Health Sciences Research*, 12(1): 39-43.
 31. Ahmadzadeh S, Asadipour A, Pournamdari M, Behnam B, Rahimi HR, Dolatabadi M. Removal of ciprofloxacin from hospital wastewater using electrocoagulation technique by aluminum electrode: Optimization and modelling through response surface methodology. *Process Safety and Environmental Protection*. 2017;109:538-47.
 32. Fouladgar M, Ahmadzadeh S. Application of a nanostructured sensor based on NiO nanoparticles modified carbon paste electrode for determination of methyl dopa in the presence of folic acid. *Applied Surface Science*. 2016;379:150-5.
 33. Pardakhty A, Ahmadzadeh S, Avazpour S, Gupta VK. Highly sensitive and efficient voltammetric determination of ascorbic acid in food and pharmaceutical samples from aqueous solutions based on nanostructure carbon paste electrode as a sensor. *Journal of Molecular Liquids*. 2016;216:387-91.
 34. Soltani H, Pardakhty A, Ahmadzadeh S. Determination of hydroquinone in food and pharmaceutical samples using a voltammetric based sensor employing NiO nanoparticle and ionic liquids. *Journal of Molecular Liquids*. 2016;219:63-7.
 35. Rezayi M, Heng LY, Kassim A, Ahmadzadeh S, Abdollahi Y, Jahangirian H. Immobilization of Ionophore and Surface Characterization Studies of the Titanium(III) Ion in a PVC-Membrane Sensor. *Sensors*. 2012;12(7):8806-14.
 36. Wang Z, Li P, Chen Y, Liu J, Zhang W, Guo Z, et al. Synthesis, characterization and electrical properties of silicon-doped graphene films. *Journal of Materials Chemistry C*. 2015;3(24):6301-6.
 37. Denis PA. Chemical Reactivity and Band-Gap Opening of Graphene Doped with Gallium, Germanium, Arsenic, and Selenium Atoms. *ChemPhysChem*. 2014;15(18):3994-4000.
 38. Schnelle W, Fischer R, Gmelin E. Specific heat capacity and thermal conductivity of NdGaO₃ and LaAlO₃ single crystals at low temperatures. *Journal of Physics D: Applied Physics*. 2001;34(6):846-51.